

# SpecGradFilter: A Spectral Gradient Filtering Framework for Taming Federated Heterogeneity

Liyang Yuan, Yibo Yang, Dandan Guo\*, Peter Richtárik, Zhouchen Lin

**Abstract**—Federated Learning (FL) is fundamentally challenged by statistical heterogeneity, where non-identically distributed (non-IID) data induces “client drift” that severely hampers global convergence. While existing approaches attempt to mitigate this drift through spatial-domain gradient correction or regularization, they overlook the intrinsic spectral structure of optimization signals. In this work, we revisit client drift from a novel frequency-domain perspective and uncover a critical “Spectral Bias of Drift”: inter-client gradient divergence is predominantly concentrated in low-frequency components which encode client-specific distributional shifts, while high-frequency components representing fine-grained features remain relatively consistent. Motivated by this, we propose SpecGradFilter, a unified Spectral Gradient Filtering Framework that tames heterogeneity by suppressing discordant low-frequency signals. Crucially, we demonstrate that SpecGradFilter is a generalizable principle, effective not only via precise FFT-based truncation but also through spatial approximations like Gaussian detrending. Extensive experiments on benchmarks such as CIFAR-10/100 and Tiny-ImageNet demonstrate that SpecGradFilter significantly performs better performance in highly Non-IID settings with negligible communication overhead, establishing a new paradigm for robust federated optimization.

**Index Terms**—Federated Learning, Non-IID Data, Client Drift, Spectral Analysis, Gradient Filtering.

## I. INTRODUCTION

FEDERATED Learning (FL) [1] has emerged as a promising paradigm for enabling collaborative machine learning across decentralized clients without sharing raw data, thereby preserving data privacy [2, 3, 4, 5]. Despite its appeal, the performance of FL is fundamentally hindered by statistical heterogeneity across clients. When local datasets are non-IID, the local optimization objectives deviate from the global objective, causing client updates toward client-specific optima. This phenomenon, commonly referred to as client drift, significantly slows down convergence and degrades the generalization performance of the global model [6, 7, 8, 9, 10, 11, 12].

To mitigate client drift, existing research has predominantly focused on spatial-domain optimization strategies. Representative approaches include constraining local update magnitudes

through proximal regularization (e.g., FedProx) [13], correcting update directions using control variates (e.g., SCAFFOLD) [14], dynamically aligning global and local objectives via regularization mechanisms (e.g., FedDyn) [10], as well as optimizing federated aggregation by dynamically weighing local updates based on dataset size and category distribution discrepancy (e.g., FedDisco) [15] or by leveraging client-level representations to adjust aggregation weights (e.g., FedAWA) [16]. While these methods have demonstrated effectiveness under certain conditions, they fundamentally treat gradients as unstructured numerical vectors in the parameter space. As a result, they implicitly assume that all gradient components contribute equally, overlooking potential structural patterns and spectral correlations within the gradients themselves.

In this work, we revisit the client drift problem from a novel frequency-domain perspective. Our investigation is inspired by the well-established spectral bias of neural networks [17, 18], which suggests that deep models tend to learn low-frequency (smooth) functions before capturing high-frequency details. In the federated setting, this bias implies that during local training on heterogeneous data, clients rapidly overfit to coarse-grained, distribution-specific patterns. Building on this intuition, we identify a critical phenomenon, which we term the Spectral Bias of Drift: inter-client gradient divergence is not uniformly distributed across the spectrum but is instead predominantly concentrated in low-frequency components. These components encode client-specific distributional shifts, such as label imbalance or background style variations, whereas high-frequency components corresponding to finer-grained features or stochastic variations remain comparatively consistent across clients.

This observation reveals a fundamental limitation of standard federated optimization schemes such as FedAvg, which aggregate client model updates without distinguishing their underlying spectral components. Since local updates implicitly encode gradient information across all frequencies, aggregating updates dominated by highly inconsistent low-frequency components inadvertently amplifies client drift and hinders global convergence. Motivated by this insight, we propose SpecGradFilter, a spectral framework for federated optimization that mitigates heterogeneity by suppressing divergent low-frequency components during local updates. SpecGradFilter targets the structural source of client drift by removing energy-dominant yet drift-prone spectral components, while preserving shared high-frequency information that is beneficial for generalization. Beyond its Fourier-based formulation, SpecGradFilter transcends as a universal optimization principle. We show that its core—low-frequency suppression—can be flexibly

Liyang Yuan is a postgraduate with the School of Artificial Intelligence, Jilin University, Changchun 130012, China. (e-mail: yuanly24@mails.jlu.edu.cn).

Yibo Yang is a Research Scientist with King Abdullah University of Science and Technology (KAUST), Thuwal, Saudi Arabia. (e-mail: yibo.yang93@gmail.com).

Dandan Guo is a Professor with the School of Artificial Intelligence, Jilin University, Changchun 130012, China. (e-mail: guodandan@jlu.edu.cn). \*Corresponding author.

Peter Richtárik is a Full Professor with the Computer Science at the King Abdullah University of Science and Technology (KAUST), Thuwal, Saudi Arabia. (e-mail: peter.richtarik@kaust.edu.sa).

Zhouchen Lin is a Professor with School of Intelligence Science and Technology, Peking University, China. (e-mail: zlin@pku.edu.cn).

instantiated through either precise spectral truncation or high-efficiency spatial operators, such as pooling-based detrending. This flexibility enables SpecGradFilter to be easily integrated into existing federated learning pipelines with minimal computational overhead. Our main contributions are summarized as follows:

- We uncover the *Spectral Bias of Drift* in FL and provide empirical evidence that client gradient divergence is dominated by low-frequency components.
- We propose SpecGradFilter, a simple yet effective framework that mitigates client drift by suppressing divergent low-frequency gradient components, with implementations in both frequency and spatial domains.
- Extensive experiments under highly Non-IID settings demonstrate that SpecGradFilter consistently achieves superior performance and convergence speed compared to a wide range of strong federated baselines.

## II. RELATED WORK

### A. Federated Learning under Data Heterogeneity

Federated Learning (FL) faces fundamental optimization challenges under data heterogeneity. Non-IID distributions induce client drift, where local updates diverge from the global trajectory due to biased objectives and multi-step local training. This effect, exacerbated by limited client participation, significantly severely hampers convergence and generalization [1, 7, 8, 19, 20].

Existing approaches to mitigating client drift can be broadly categorized into local objective regularization and modified aggregation strategies. Local regularization aims to align local updates with the global objective. Representative works include FedProx [13], which introduces an  $\ell_2$  proximal term to constrain model deviation, and FedDyn [10], which employs dynamic regularization for update consistency. Alternatively, SCAFFOLD [14] utilizes control variates to explicitly correct gradient bias. Recent refinements further explore auxiliary variables to track parameter discrepancies (e.g., FedDC [21]) or calibrate loss functions to address label skew (e.g., FedLC [22]). Another line of research optimizes server-side aggregation. Methods such as FedLAW [23], FedAWA [16], and FedDisco [15] redesign aggregation weights by accounting for data imbalance, client representations, or distribution discrepancies. Furthermore, InCo [24] leverages cross-layer information to enhance deeper layer alignment without extra communication. While these approaches are effective, most of them operate in the parameter or gradient value space, emphasizing magnitude, direction, or statistical weighting of updates. In contrast, relatively little attention has been paid to the structural properties of gradients themselves, particularly from a frequency-domain perspective, which motivates our work.

### B. From Spectral Bias to Frequency-Domain Optimization

The spectral behavior of deep neural networks has been extensively studied under the framework of spectral bias or the Frequency Principle. Early theoretical and empirical analyses show that neural networks tend to learn target

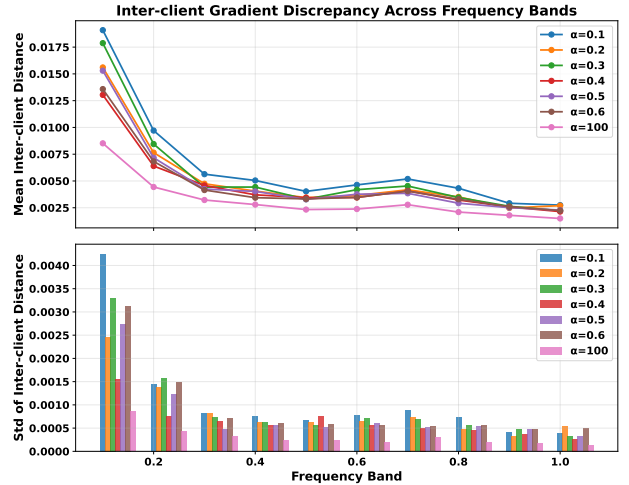


Fig. 1. Client gradient divergence across frequency bands under different heterogeneous distributions (Dirichlet hyperparameter  $\alpha$ ). Top: Mean inter-client distance showing drift magnitude. Bottom: Standard deviation showing drift instability. Results are obtained from ResNet-20 on CIFAR-10, with gradients collected every 30 rounds, for a total of four times.

functions from low-frequency components to high-frequency ones during training [17, 18]. Lower-frequency components are not only learned earlier but are also more robust to parameter perturbations, revealing an implicit bias in deep optimization dynamics. However, we argue that in federated contexts, this rapid capture of low-frequency information can be double-edged, as these components are also most susceptible to absorbing discordant, client-specific distributional biases.

Several recent works have introduced frequency-domain techniques into federated or distributed learning, primarily motivated by communication efficiency. For instance, SuperNeurons [25] and FedFD [26] apply FFT-based filtering or sparsification to reduce transmission costs by targeting low-energy or noisy components. Similarly, FedFT [27] utilizes the Discrete Cosine Transform (DCT) for compact parameter representation and flexible updates. Despite their effectiveness, these methods are largely designed as compression or acceleration techniques, where frequency filtering is guided by energy or sparsity considerations rather than optimization stability. In contrast, our method leverages frequency-domain filtering as a regularization mechanism to directly mitigate client drift. By suppressing energy-dominant yet drift-prone low-frequency signals, we prioritize optimization alignment over mere data compression.

## III. UNDERSTANDING CLIENT DRIFT VIA SPECTRAL LENS IN FEDERATED LEARNING

### A. Preliminaries

Federated Learning is a distributed learning paradigm that enables collaborative model training over data from  $K$  clients without centralizing their private datasets  $\mathcal{D}_{1:K}$ . A central server coordinates the optimization process by aggregating model

updates from participating clients, whose learning objective is to minimize the global empirical risk

$$\begin{aligned} F(w) &= \frac{1}{K} \sum_{k=1}^K f_k(w), \\ f_k(w) &= \frac{1}{|\mathcal{D}_k|} \sum_{(x,y) \in \mathcal{D}_k} \mathcal{L}_k(w; x, y), \end{aligned} \quad (1)$$

where  $f_k(w)$  denotes the local objective defined on client  $k$ 's data,  $w$  means the to-be-learned parameter. The most widely adopted optimization algorithm for FL is FedAvg [1], which proceeds in iterative communication rounds. In  $t$ -th round, the server (1) broadcasts the current global model  $w^t$  to a subset of clients. The  $k$ -th client then performs several steps of (2) local training on its private data, producing an updated local model  $w_k^{t+1}$ . These local models are subsequently (3) uploaded to the server and (4) aggregated to form the next global model:  $w^{t+1} = \sum_k \frac{1}{K} w_k^{t+1}$ .

Despite its success, the fundamental challenge in FL is client drift. Mathematically, let  $g_k = \nabla f_k(w)$  be the local gradient and  $g = \nabla F(w)$  be the global gradient. Due to the Non-IID nature of local datasets  $\mathcal{D}_k$ , the local update direction often deviates from the global optimum:

$$\Delta_k = \|g_k - g\|, \quad (2)$$

where  $\Delta_k$  represents the magnitude of the drift. Prior research typically views  $\Delta_k$  as an unstructured numerical error in the spatial domain. However, this perspective overlooks the internal structural properties of the model parameters. We raise a question: *Is this drift uniformly distributed across the internal components of the parameter vector? If we transform this deviation into the frequency domain, what patterns will emerge?*

### B. Our Observation: Spectral Bias of Drift

To formally analyze the structural properties of client drift, we interpret the flattened gradient vector  $\mathbf{g}_l \in \mathbb{R}^{d_l}$  of the  $l$ -th layer as a discrete signal and project it into the frequency domain via a real-valued Discrete Fourier Transform ( $\mathcal{F}$ ), denoted as:

$$\hat{\mathbf{g}}_l = \mathcal{F}(\mathbf{g}_l) \in \mathbb{C}^{\lfloor d_l/2 \rfloor + 1}. \quad (3)$$

We then partition the spectrum into  $M$  disjoint frequency bands  $\{\mathcal{B}_m\}_{m=1}^M$  with a set of binary masks  $\{M_m\}_{m=1}^M$ . Let  $\delta_{l,m}^{(j,k)} = \|\hat{\mathbf{g}}_l^j \odot M_m - \hat{\mathbf{g}}_l^k \odot M_m\|_2$  represent the spectral distance between client  $j$  and client  $k$  in frequency band  $m$  at layer  $l$ . To quantify the collective divergence and its stability across the system, we define the following metrics averaged over all  $L$  layers and  $N_p = \binom{K}{2}$  client pairs:

$$\begin{aligned} \text{Dist}(m) &= \frac{1}{L \cdot N_p} \sum_{l=1}^L \sum_{1 \leq j < k \leq K} \delta_{l,m}^{(j,k)}, \\ \text{Std}(m) &= \sqrt{\frac{1}{L \cdot N_p} \sum_{l=1}^L \sum_{1 \leq j < k \leq K} \left( \delta_{l,m}^{(j,k)} - \text{Dist}(m) \right)^2}, \end{aligned} \quad (4)$$

where  $\text{Dist}(m)$  denotes the mean Inter-client distance which reflects the expected magnitude of spectral divergence, and

$\text{Std}(m)$  provides its standard deviation, capturing the fluctuation of these pairwise discrepancies across the population.

We conducted experiments on the CIFAR-10 dataset using ResNet-20 as the base model, where we simulated heterogeneous data distributions by partitioning the training data across clients according to a Dirichlet distribution, with concentration parameter  $\alpha$ , where smaller values of  $\alpha$  correspond to higher degrees of data heterogeneity. During training stage, we perform rFFT on the flattened client gradient vector and compute inter-client distances and variances within each frequency band ( $M=10$ ) and averaged them across layers.

As illustrated in Figure 1, a striking pattern emerges: both the mean distance and the standard deviation of client drift are predominantly concentrated in the low-frequency bands, while high-frequency components remain relatively consistent across clients. Crucially, we observe a non-linear sensitivity to data heterogeneity: as the Dirichlet parameter  $\alpha$  decreases from 0.6 to 0.1, the low-frequency drift exhibits a super-linear surge in both magnitude and variance, whereas the high-frequency components remain remarkably stable and insensitive to the degree of statistical skew. This discovery reveals a critical structural property of federated optimization, which we term the **Spectral Bias of Drift**: the systematic divergence induced by non-IID data is not an unstructured numerical noise, but is instead encoded primarily within the smooth, globally correlated variations that form the semantic backbone of the model. This insight suggests that increasing heterogeneity primarily ‘‘attacks’’ these low-frequency components, causing local optimization trajectories to fragment and diverge explosively. Such spectral concentration underscores the necessity of frequency-selective intervention, as targeted suppression of these discordant low-frequency signals can effectively realign fragmented local updates toward a shared consensus with minimal impact on essential features.

### C. Pilot Study about Spectral Suppression

Building on the observation that client drift is frequency-dependent, we conduct a pilot study to investigate whether targeted intervention in the spectral domain can effectively realign local updates. To investigate the impact of spectral modulation, we consider a gradient modulation operator  $\Phi$  that maps the original gradient to a transformed version. We measure the mean layer-wise divergence  $\Delta_l(\Phi)$  as the average distance between transformed local updates and their collective consensus  $\bar{\mathbf{g}}_l = \frac{1}{K} \sum_k \mathbf{g}_l^k$ :

$$\Delta_l(\Phi) = \frac{1}{K} \sum_{k=1}^K \|\Phi(\mathbf{g}_l^k) - \Phi(\bar{\mathbf{g}}_l)\|_2. \quad (5)$$

We examine two representative cases: (1)  $\Phi$  is the identity mapping (i.e.,  $\Phi(\mathbf{g}_l^k) = \mathbf{g}_l^k$ ), corresponding to the standard FedAvg baseline; and (2)  $\Phi$  is an ideal high-pass filter that suppresses the low-frequency components of  $\mathbf{g}_l^k$  identified in subsection III-B.

We visualize the divergences for a ResNet-20 model on CIFAR-10 ( $\alpha = 0.1$ ). As shown in Figure 2, applying low-frequency suppression significantly reduces the mean divergence across all layers. This reduction is mathematically

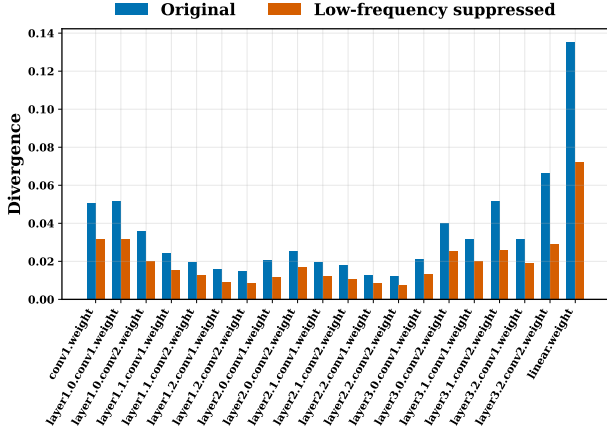


Fig. 2. Layer-wise client gradient divergence before and after low-frequency suppression at the 30th communication round on CIFAR-10 using ResNet-20, with Dirichlet ( $\alpha = 0.1$ ).

consistent with the findings in subsection III-B: by removing the low-frequency components that exhibit the highest pairwise discrepancy ( $\text{Dist}(m)$  and  $\text{Std}(m)$ ), the residual gradient signals become naturally more aligned. Notably, the most pronounced improvements occur in the deeper convolutional and final classification layers, which we identified as being most vulnerable to client-specific distribution shifts.

#### IV. METHODOLOGY

Motivated by the Spectral Bias of Drift observed in above Section, we propose SpecGradFilter, a unified framework designed to tame federated heterogeneity by selectively suppressing drift-prone spectral components. The core of our framework is the spectral modulation operator  $\Phi$ , which serves as a structured regularizer to align local updates across clients. The overall workflow of SpecGradFilter integrated with FedAvg is illustrated in Fig. 3.

##### A. Realizations of the Spectral Filtering Operator

While  $\Phi$  represents a generic high-pass operation, its most precise realization is achieved in the frequency domain. Let  $\mathbf{g}_l^k \in \mathbb{R}^{d_l}$  denote the flattened gradient of client  $k$  at layer  $l$ . The spectral filtering process is formally defined as:

$$\Phi(\mathbf{g}_l^k) = \mathcal{F}^{-1}(\mathcal{H}_r \odot \mathcal{F}(\mathbf{g}_l^k)), \quad (6)$$

where  $\mathcal{F}$  and  $\mathcal{F}^{-1}$  denote the real-valued Discrete Fourier Transform (rFFT) and its inverse, respectively.  $\mathcal{H}_r$  is a spectral mask characterized by the suppression ratio  $r \in [0, 1)$ . This layer-wise treatment ensures that the spectral modulation is adaptive to the parameter scale and topology of each layer.

Following our empirical findings that drift predominantly resides in low frequencies, we instantiate  $\mathcal{H}_r$  as a high-pass filter. Specifically, let  $\mathbf{z} = \mathcal{F}(\mathbf{g}_l^k) \in \mathbb{C}^{\lfloor d_l/2 \rfloor + 1}$  be the vector of spectral coefficients. The mask  $\mathcal{H}_r \in \{0, 1\}^{\lfloor d_l/2 \rfloor + 1}$  is defined to zero out the first  $\lfloor r \cdot (\lfloor d_l/2 \rfloor + 1) \rfloor$  low-frequency components:

$$[\mathcal{H}_r]_m = \begin{cases} 0, & m < \lfloor r \cdot (\lfloor d_l/2 \rfloor + 1) \rfloor, \\ 1, & \text{otherwise,} \end{cases} \quad (7)$$

where  $m$  denotes the frequency index. By applying this spectral mask, the operator  $\Phi(\mathbf{g}_l^k)$  effectively attenuates client-specific distributional shifts while preserving shared semantic features.

**Local Update with Spectral Filtering.** During each communication round  $t$ , once a client  $k$  is sampled, it performs  $E$  local epochs of optimization. To rectify the optimization trajectory in real-time, the spectral operator  $\Phi$  is applied to the local gradient at each step. Formally, for each layer  $l$ , the parameters are updated as follows:

$$\mathbf{w}_l^{k,(t,e+1)} = \mathbf{w}_l^{k,(t,e)} - \eta \Phi(\mathbf{g}_l^{k,(t,e)}), \quad (8)$$

where  $\eta$  is local learning rate and  $\mathbf{w}_l^{k,(t,0)} = \mathbf{w}_l^{(t)}$  is the global model parameter received from the server. Intuitively, by applying  $\Phi$  into the local update loop, SpecGradFilter continuously filters out the client-specific low-frequency “noise” that would otherwise accumulate into significant drift. It ensures that the local models remain within a proximity that favors stable global aggregation, effectively taming the heterogeneity-induced divergence at its source. Crucially, this design renders SpecGradFilter a plug-and-play module: it seamlessly integrates into standard FL frameworks by simply applying  $\Phi$  before the local update. Please see our algorithm in Algorithm 1.

**Generalizing to Spatial-Domain Realizations.** To demonstrate the versatility of our spectral filtering principle, we provide alternative realizations of  $\Phi$  that operate directly in the spatial domain. Inspired by signal processing, the low-frequency components (representing the “trend” or client-specific bias) can be effectively captured via local smoothing kernels without explicit frequency transformation. Specifically, we instantiate  $\Phi$  using Local Average Pooling Detrend (LAP-D) or Gaussian Detrend (GD), defined as  $\Phi(\mathbf{g}_l^k) = \mathbf{g}_l^k - \text{Smooth}(\mathbf{g}_l^k)$ . Here,  $\text{Smooth}(\cdot)$  acts as a spatial low-pass filter that extracts the coarse-grained drift, where details are provided in Section I of the supplementary material. By subtracting this trend, these variants achieve a high-pass effect equivalent to our frequency-domain mask. This provides a unified spatial-domain optimization pipeline, which is particularly advantageous for hardware environments where convolution primitives are more optimized than Fourier transforms, while ensuring strict linear-time complexity  $\mathcal{O}(d_l)$ .

##### B. The Spectral Preconditioning View

The proposed frequency-domain filtering can also be interpreted from a preconditioning perspective. Specifically, the rFFT-based suppression constitutes a linear projection in the spectral Hilbert space. Let  $\mathbf{D} = \text{diag}(\mathcal{H}_r)$  be the diagonal mask matrix constructed from the spectral mask defined in Eq. 7. The filtered gradient can be equivalently written as:

$$\tilde{\mathbf{g}} = \mathcal{F}^{-1} \mathbf{D} \mathcal{F}(\mathbf{g}) = \mathbf{P}_{\text{spec}} \mathbf{g}, \quad (9)$$

where  $\mathbf{P}_{\text{spec}} = \mathcal{F}^{-1} \mathbf{D} \mathcal{F}$  is the spectral projection preconditioner. Unlike classical preconditioners that aim to correct curvature-induced ill-conditioning (e.g., second-order or adaptive methods),  $\mathbf{P}_{\text{spec}}$  targets ill-conditioning arising from statistical heterogeneity across clients. As shown in our empirical analysis, heterogeneity-induced gradient discrepancies

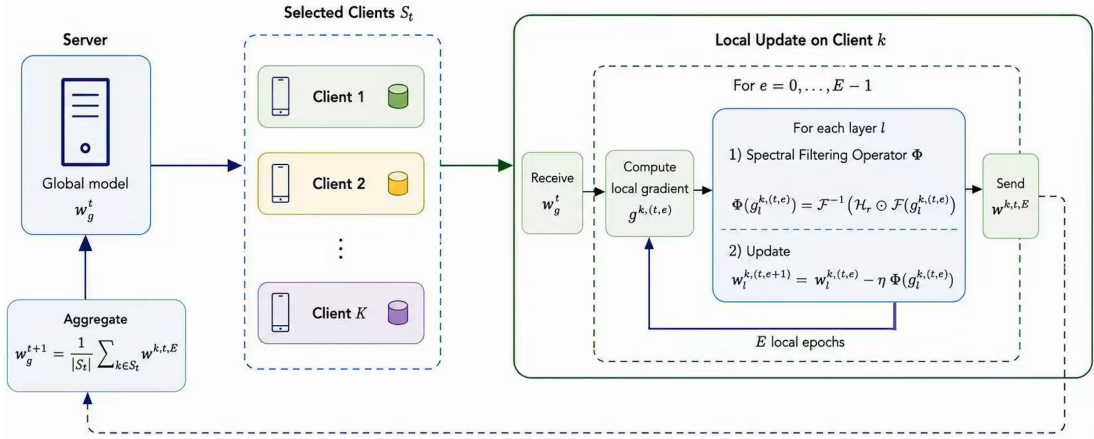


Fig. 3. Overview of the proposed SpecGradFilter framework integrated with FedAvg. The figure illustrates the overall training pipeline including local spectral gradient filtering, client updates, and server-side aggregation.

---

### Algorithm 1 SpecGradFilter with FedAvg

---

- 1: **Input:** Communication rounds  $T$ , local epochs  $E$ , local learning rate  $\eta$ , low-frequency filtering ratio  $r$
  - 2: **Output:** Global model  $w_g^T$
  - 3: Initialize global model  $w_g^0$
  - 4: **for**  $t = 0$  **to**  $T - 1$  **do**
  - 5:   Randomly select active client set  $S_t$
  - 6:   **for** each client  $k \in S_t$  **in parallel do**
  - 7:      $w^{k,t,0} \leftarrow w_g^t$
  - 8:     **for**  $e = 0$  **to**  $E - 1$  **do**
  - 9:       Compute local gradient  $g^{k,t,e} \leftarrow \nabla \mathcal{L}_k(w^{k,t,e})$
  - 10:       **for** each layer  $l$  in model **do**
  - 11:          Compute  $\Phi(g_l^{k,(t,e)})$  via Eq. 6
  - 12:          Update  $w_l^{k,(t,e+1)}$  via Eq. 8
  - 13:       **end for**
  - 14:     **end for**
  - 15:     Send  $w^{k,t,E}$  to server
  - 16:   **end for**
  - 17:    $w_g^{t+1} \leftarrow \frac{1}{|S_t|} \sum_{k \in S_t} w^{k,t,E}$
  - 18: **end for**
  - 19: **return**  $w_g^T$
- 

are highly anisotropic and predominantly concentrated in low-frequency subspaces. Projecting gradients away from these subspaces therefore improves inter-client alignment without requiring curvature estimation.

### C. Theoretical Analysis

We provide a convergence guarantee for our method under standard smoothness and stability assumptions.

**Theorem IV.1** (Convergence of SpecGradFilter). *Under Assumptions in Section II of the supplementary material, with learning rate  $\eta = \frac{1}{\sqrt{TEL}}$  and  $E$  local epochs per round,*

*SpecGradFilter satisfies:*

$$\frac{1}{T} \sum_{t=0}^{T-1} \mathbb{E} \left[ \|\nabla F(w^t)\|^2 \right] \leq \frac{2(F(w^0) - F^*)}{\sqrt{T}} + \frac{C_1}{\sqrt{T}} + C_2 E^2 \eta^2 L^2 \delta_{\text{high}}^2. \quad (10)$$

where  $C_1$  and  $C_2$  are constants depending on  $\sigma^2$  and  $\rho$ , and  $F^* = \min_{\mathbf{w}} F(\mathbf{w})$ .

The detailed proof is provided in Section II of the supplementary material.

a) *Discussion.*: The bound indicates that SpecGradFilter achieves an  $\mathcal{O}(1/\sqrt{T})$  convergence rate for non-convex objectives. The additional term  $C_2 E^2 \eta^2 L^2 \delta_{\text{high}}^2$  quantifies the bias introduced by high-frequency gradient filtering.

## V. EXPERIMENTS

### A. Experimental Setups

**Datasets.** We evaluate our methods on three widely used image classification benchmarks: CIFAR-10 [28], CIFAR-100 [28], and Tiny-ImageNet [29]. These datasets vary in complexity, number of classes, and dataset size, providing a comprehensive evaluation of the robustness and generalization of federated learning algorithms. Specifically, CIFAR-10 contains 60,000 color images of size  $32 \times 32$  pixels across 10 classes, with 50,000 training images and 10,000 test images. CIFAR-100 has the same total number of images but includes 100 classes, with 500 training images and 100 test images per class, making it a more challenging benchmark due to the increased number of classes and finer-grained categories. Tiny-ImageNet is a subset of the ImageNet dataset, consisting of 200 classes, each with 500 training images, 50 validation images, and 50 test images, with images resized to  $64 \times 64$  pixels. Its larger number of classes and higher-resolution images present a significantly more challenging scenario for federated learning.

To simulate realistic data heterogeneity across clients, we adopt a Dirichlet distribution-based partitioning strategy. Specifically, for each dataset, we sample class distributions

TABLE I

TEST ACCURACY (%) ON CIFAR-10, CIFAR-100, AND TINY-IMAGENET UNDER VARYING NON-IID SETTINGS USING RESNET-20 WITH 100 CLIENTS, A CLIENT PARTICIPATION RATIO OF 0.1, AND A FIXED COMMUNICATION BUDGET OF 300 ROUNDS. RESULTS ARE REPORTED AS MEAN  $\pm$  STANDARD DEVIATION OVER THREE RUNS WITH DIFFERENT RANDOM SEEDS.

Method	CIFAR-10		CIFAR-100		Tiny-ImageNet	
	$\alpha = 0.6$	$\alpha = 0.1$	$\alpha = 0.6$	$\alpha = 0.1$	$\alpha = 0.6$	$\alpha = 0.1$
FedAvg	77.02 $\pm$ 0.79	58.40 $\pm$ 1.30	35.37 $\pm$ 0.89	28.88 $\pm$ 0.42	31.22 $\pm$ 0.24	25.82 $\pm$ 0.74
FedProx	77.01 $\pm$ 0.36	58.29 $\pm$ 0.85	36.60 $\pm$ 1.81	28.29 $\pm$ 0.72	31.94 $\pm$ 0.74	25.47 $\pm$ 0.76
FedDyn	82.18 $\pm$ 0.22	69.34 $\pm$ 1.62	42.78 $\pm$ 1.47	34.54 $\pm$ 1.46	35.14 $\pm$ 0.12	30.32 $\pm$ 0.34
SCAFFOLD	78.23 $\pm$ 0.66	56.00 $\pm$ 2.40	40.04 $\pm$ 0.67	28.83 $\pm$ 0.63	34.87 $\pm$ 0.62	27.18 $\pm$ 0.49
FedCM	84.03 $\pm$ 0.21	66.55 $\pm$ 1.73	38.25 $\pm$ 2.92	28.24 $\pm$ 0.92	22.59 $\pm$ 0.52	14.33 $\pm$ 1.44
FedSAM	75.88 $\pm$ 0.13	57.05 $\pm$ 0.51	35.59 $\pm$ 0.49	27.52 $\pm$ 0.39	29.56 $\pm$ 2.44	25.56 $\pm$ 0.11
FedDisco	76.71 $\pm$ 0.66	58.40 $\pm$ 0.92	36.27 $\pm$ 1.25	27.87 $\pm$ 0.58	32.30 $\pm$ 1.24	25.76 $\pm$ 0.42
FedAWA	76.49 $\pm$ 0.55	58.11 $\pm$ 1.14	36.10 $\pm$ 1.05	28.12 $\pm$ 0.46	31.94 $\pm$ 0.91	25.65 $\pm$ 0.30
FedLWS	76.77 $\pm$ 0.80	58.29 $\pm$ 0.55	36.33 $\pm$ 1.28	27.84 $\pm$ 0.38	31.64 $\pm$ 0.06	25.73 $\pm$ 0.19
<b>Ours</b>	<b>85.11 <math>\pm</math> 0.11</b>	<b>78.05 <math>\pm</math> 1.88</b>	<b>45.99 <math>\pm</math> 1.12</b>	<b>40.16 <math>\pm</math> 0.64</b>	<b>36.73 <math>\pm</math> 0.38</b>	<b>31.55 <math>\pm</math> 0.19</b>

for each client from a Dirichlet distribution parameterized by  $\alpha \in 0.1, 0.6$ . A smaller  $\alpha$  value corresponds to more non-IID distributions, meaning that individual clients receive highly skewed subsets of classes, reflecting the imbalanced and biased data often observed in real-world federated scenarios. Conversely, a larger  $\alpha$  value leads to more IID-like distributions, where each client’s local dataset more closely approximates the overall class distribution. To illustrate the severity of data heterogeneity under the highly non-IID setting, Figure 1 of the supplementary material visualizes the client-wise class distributions of CIFAR-10, CIFAR-100, and Tiny-ImageNet under Dirichlet partitions with  $\alpha = 0.1$  and  $\alpha = 0.6$ . Each heatmap illustrates the proportion of samples per class for each client, where the horizontal axis corresponds to client indices and the vertical axis represents class IDs. As expected, the  $\alpha = 0.1$  setting exhibits highly skewed and imbalanced data allocations: certain clients show dark, concentrated regions indicating dominance of only a few classes, while other classes may be nearly absent. This reflects a strongly non-IID scenario commonly observed in real-world FL applications. In contrast, when  $\alpha = 0.6$ , the heatmaps become noticeably smoother with reduced color variations, indicating that clients receive more balanced class distributions and the overall data heterogeneity is significantly alleviated. These two complementary visualizations allow us to systematically assess the behavior and robustness of different federated learning algorithms across varying levels of client data heterogeneity. Besides, we also use realistic FL dataset-FEMNIST [30], medical imaging dataset-BloodMNIST [31] and NLP dataset-Yahoo! Answers as our benchmarks.

**Baselines.** We compare our approach with several representative federated learning algorithms, including: (1) **FedAvg** [1], the standard federated learning algorithm; (2) **FedProx** [13], which introduces a proximal term to mitigate client drift under data heterogeneity; (3) **FedDyn** [10], which employs dynamic regularization to correct local update bias; (4) **SCAFFOLD** [14], which uses control variates to reduce gradient variance; (5) **FedCM** [32], which enhances federated averaging by incorporating client-level momentum to correct

local update bias and improve stability. (6) **FedSAM** [33, 34], which integrates sharpness-aware minimization into federated optimization; (7) **FedDISCO** [15], which optimizes federated aggregation by dynamically weighing local updates based on both dataset size and category distribution discrepancy; (8) **FedAWA** [16], which optimizes aggregation weights based on client-level representations; and (9) **FedLWS** [35], which applies a shrinkage operation on aggregation weights.

**Implementation Details.** We primarily adopt ResNet-20 [36] as the backbone. Following [37, 38], all Batch Normalization (BN) layers are replaced with Group Normalization (GN) [39] to enhance stability under data heterogeneity. We also evaluate ResNet-18, WideResNet-56\_2, DenseNet-121, and ViT as additional backbones. Unless otherwise specified, we use the FFT-based realization as the default implementation of SpecGradFilter. For the federated learning process, we conduct 300 communication rounds with a client participation rate of 0.1. Each activated client performs 5 local epochs per round using an SGD optimizer. All methods share the same base protocol: 100 clients in total, active client ratio 0.1, batch size 50, and weight decay 0.001.

To ensure a fair and rigorous comparison, we carefully tune the learning rate and method-specific hyperparameters for every baseline via grid search. Specifically, we perform (at minimum) a 2D grid over the base learning rate  $lr \in \{0.01, 0.05, 0.1, 0.15\}$  combined with 5 representative values of each method’s specific parameter. For FedAvg and SCAFFOLD (which have no extra hyperparameters), we conduct an extensive 1D search over a wider learning rate range  $\{0.01, 0.02, \dots, 0.2\}$ . If the optimum lies on a boundary or a plateau is observed, we adaptively expand the grid outward until the peak is fully enclosed by strictly lower performance on all surrounding sides. This guarantees that every baseline is evaluated at its verified interior optimum.

The final optimal hyperparameter configurations obtained after this search are shown in Table 1 of the supplementary material. For our method, we use spectral filter ratio  $r = 0.05$ . These configurations (including the tuned baselines) are kept consistent across different datasets and backbone networks

unless otherwise stated.

## B. Main Results

**Comparison with Baseline Methods.** Table I reports the test accuracy under different degrees of data heterogeneity. Overall, our method consistently achieves the best performance across all datasets and Non-IID settings, demonstrating strong robustness to client drift. The performance gains are especially pronounced under severe heterogeneity ( $\alpha = 0.1$ ) on CIFAR-10 and CIFAR-100, where our method significantly surpasses both FedAvg and strong drift-mitigation baselines. This trend aligns well with our empirical findings that client gradient divergence is dominated by low-frequency components under strong statistical heterogeneity, and that suppressing these components before local updates effectively improves update alignment across clients. Beyond final accuracy, our method also exhibits substantially faster convergence. As shown in Figure 5, it reaches high accuracy much earlier than competing methods, particularly on CIFAR-10 and CIFAR-100 with  $\alpha = 0.1$ , indicating that frequency-based gradient filtering not only stabilizes training but also accelerates global optimization within a fixed communication budget.

**Combination with FL Methods under Different Backbones.** Table II reports test accuracy on CIFAR-10/100 under a highly heterogeneous setting ( $\alpha = 0.1$ ) across different model backbones. For ViT, low-frequency suppression is applied only to the patch embedding gradients, since client-specific discrepancies are empirically found to be pronounced in the low-frequency components at this stage. For FedProx and SCAFFOLD, the proposed filtering is applied only to the data-driven gradient components, while their method-specific correction terms (e.g., the proximal regularizer in FedProx and the control variate updates in SCAFFOLD) are left unchanged to preserve the original algorithmic structure. Ours consistently improves performance when integrated with various FL algorithms, across convolutional networks of different depths (ResNet20/18, WideResNet56\_2, DenseNet121) as well as transformer-based models (ViT). These results demonstrate the generalizability of our method across diverse architectures. While the performance gains on ViT are more moderate compared to CNN-based models (likely due to the distinct spectral characteristics of self-attention mechanisms versus convolutions), the consistent improvement confirms that our spectral filtering principle remains effective regardless of the specific architectural inductive bias. On CIFAR-100, where heterogeneity and task complexity are more pronounced, the improvements are particularly significant for high-capacity models, supporting our motivation that suppressing client-specific low-frequency gradients leads to more stable and aligned updates. Furthermore, the learning curves in (Figure 6) show that integrating ours consistently accelerates convergence, achieving substantially higher accuracy within the same communication rounds. Collectively, these results validate that SpecGradFilter can be seamlessly integrated with various FL algorithms and backbones.

## C. Mechanism and Empirical Understanding

**Ablation on Filtering Strategy.** To validate our hypothesis that inter-client inconsistency is predominantly encoded in low-frequency gradient components, we conduct a comprehensive ablation study. We compare our proposed Low-Frequency Suppression strategies (including the FFT-based realization with a 5% cutoff and the spatial variants LAP-D/GD) against counter-intuitive baselines: High-Frequency Suppression (removing the top 5% frequencies), Random Suppression, and  $\ell_2$ -norm Rescaling (see Section I of the supplementary material for detailed settings). As shown in Table III, only strategies explicitly targeting low-frequency components yield substantial performance gains. Both LAP-D and GD significantly outperform FedAvg, confirming that removing smooth, client-specific gradient trends is critical for mitigating drift. In stark contrast, suppressing high-frequency components degrades performance, suggesting that high-frequency signals contain fine-grained discriminative features essential for generalization. Furthermore, the limited improvement of  $\ell_2$ -norm rescaling indicates that client drift is a structural spectral issue rather than merely a magnitude disparity. Notably, our FFT-based low-frequency suppression achieves the best overall accuracy on CIFAR-10 and remains highly competitive on CIFAR-100, empirically corroborating that low-frequency components are indeed the primary source of federated heterogeneity.

**Representation Alignment via CKA.** To validate whether ours promotes structural consensus among clients, we visualize the Centered Kernel Alignment (CKA) similarity of the penultimate layer representations between pairwise local models (Figure 7). While FedAvg exhibits low CKA scores (indicating that non-IID data drives clients to learn disjoint, distinct features), SpecGradFilter maintains consistently high CKA similarity across all layers. This suggests that by filtering out the low-frequency gradients which we identified as the carrier of client-specific bias, SpecGradFilter prevents the local models from diverging into incompatible feature spaces. Instead, it forces all clients to converge towards a shared, globally aligned representational structure, ensuring that the aggregated global model is constructed from semantically consistent local updates rather than conflicting ones.

**Why Does Flattening Order Matter?** Our default implementation performs a 1D FFT on flattened convolutional kernels following the natural contiguous tensor layout:

$$[\text{Out}, \text{In}, \text{H}, \text{W}],$$

which we denote as order 0123. A natural question is whether the effectiveness of SpecGradFilter depends on this flattening strategy, or whether any arbitrary permutation would produce similar behavior.

To investigate this, we systematically evaluate multiple tensor flattening orders as well as a completely random permutation under the challenging Non-IID setting ( $\alpha = 0.1$ ). The results are summarized in Table IV.

a) *Semantic Locality Matters:* Randomly permuting the flattened indices almost completely destroys the performance gain, reducing accuracy to a level comparable with or even worse than FedAvg. This observation suggests that SpecGradFilter does not function as a generic noise regularizer. Instead,

TABLE II  
PERFORMANCE COMPARISON OF FEDERATED LEARNING METHODS BEFORE AND AFTER INTEGRATING OUR METHOD ACROSS DIFFERENT BACKBONES ON CIFAR-10 AND CIFAR-100 WITH  $\alpha = 0.1$ .

Method	CIFAR-10					CIFAR-100				
	R20	R18	WRN	Dense121	ViT	R20	R18	WRN	Dense121	ViT
FedAvg	57.09	71.28	57.17	63.97	43.05	29.15	38.22	30.54	34.84	23.11
<b>+ Ours</b>	<b>78.67</b>	<b>75.88</b>	<b>76.07</b>	<b>79.64</b>	<b>45.16</b>	<b>40.87</b>	<b>44.48</b>	<b>50.94</b>	<b>52.05</b>	<b>24.02</b>
FedProx	59.44	71.55	56.91	64.26	42.71	28.54	37.93	29.41	34.58	22.86
<b>+ Ours</b>	<b>77.64</b>	<b>75.91</b>	<b>75.86</b>	<b>78.52</b>	<b>45.04</b>	<b>41.81</b>	<b>44.67</b>	<b>51.75</b>	<b>53.03</b>	<b>24.00</b>
SCAFFOLD	57.69	73.81	52.39	63.37	40.64	29.00	43.44	29.38	39.92	22.90
<b>+ Ours</b>	<b>79.08</b>	<b>78.17</b>	<b>77.86</b>	<b>85.98</b>	<b>43.56</b>	<b>46.75</b>	<b>49.32</b>	<b>58.26</b>	<b>64.03</b>	<b>24.08</b>
FedAWA	59.66	71.34	54.72	63.13	42.37	28.70	38.27	30.31	34.98	23.15
<b>+ Ours</b>	<b>77.97</b>	<b>75.92</b>	<b>76.87</b>	<b>79.59</b>	<b>45.27</b>	<b>41.44</b>	<b>44.73</b>	<b>50.95</b>	<b>51.91</b>	<b>24.01</b>

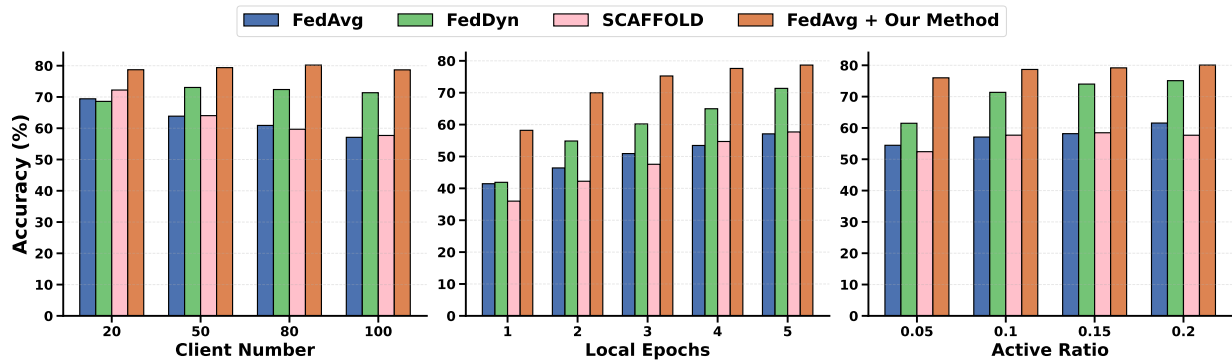


Fig. 4. Comparison between our method and FedAvg on CIFAR-10 ( $\alpha = 0.1$ ) under different federated learning configurations. The default setting uses 100 clients, 5 local epochs, and 0.1 participation rate, with each ablation varying only the corresponding hyperparameter.

TABLE III  
ABLATION OF DIFFERENT FILTERING STRATEGIES ON CIFAR-10 AND CIFAR-100 UNDER DIRICHLET ( $\alpha = 0.1$ ).

Filtering Strategy	CIFAR10	CIFAR100
None (FedAvg)	57.09	29.15
High-frequency suppression	59.99	28.31
Random suppression	58.89	28.74
$\ell_2$ -norm rescaling	59.33	27.04
Local Average Pooling Detrend	75.85	35.35
Gaussian Detrend	<b>77.06</b>	<b>41.53</b>
Low-frequency suppression	<b>78.67</b>	<b>40.87</b>

its effectiveness critically depends on preserving meaningful structural locality in parameter space.

*b) Why Do Natural Orders Work Better:* We hypothesize that client drift in federated learning primarily manifests as a macro-level cross-channel discrepancy rather than purely local spatial perturbations. Flattening orders such as 0123, 0231, and 0312 place the output-channel dimension near the outermost traversal order, causing inter-channel discrepancies to appear as slowly varying low-frequency patterns in the flattened spectrum.

Under this representation, client-specific drift becomes concentrated in low-frequency components and can therefore be effectively removed by high-pass spectral filtering, while fine-grained intra-kernel spatial structures remain preserved in higher frequencies.

TABLE IV  
IMPACT OF FLATTENING ORDER ON CONVOLUTIONAL LAYERS UNDER SEVERE HETEROGENEITY ( $\alpha = 0.1$ ). TENSOR DIMENSIONS FOLLOW THE CONVENTION [OUT, IN, H, W].

Method	CIFAR-10	CIFAR-100
FedAvg	57.09	29.15
0123 (ours)	<b>78.67</b>	<b>40.87</b>
0231	76.39	39.92
0312	75.75	39.10
3210	56.18	26.39
1230	57.17	26.22
2130	56.69	26.28
2310	56.98	25.82
2D FFT	74.93	31.96
Random after flatten	58.18	28.35

In contrast, orders such as 2310 or 3210 place the output-channel dimension at the innermost traversal position. This rearrangement converts smooth cross-channel discrepancies into rapidly oscillating high-frequency patterns. As a result, the harmful drift is no longer captured in the low-frequency spectrum and therefore bypasses the spectral filter entirely, leading to performance even below FedAvg.

*c) Comparison with 2D FFT:* We further implement a structure-preserving 2D FFT variant that independently applies spectral filtering to each spatial convolution kernel. Although the 2D FFT version still improves over FedAvg, it consistently

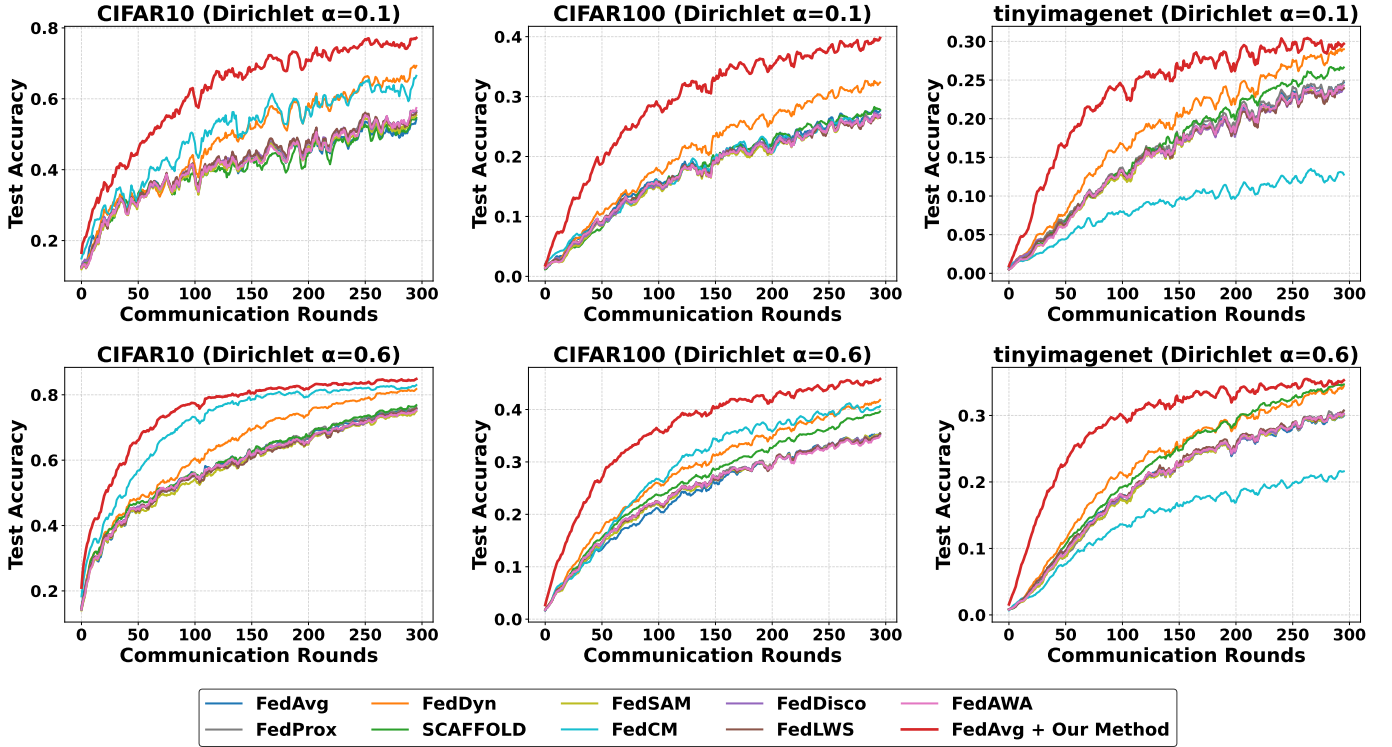


Fig. 5. Test accuracy comparisons of different federated learning methods across datasets and Dirichlet  $\alpha$  settings on ResNet20.

underperforms our 1D SpecGradFilter, especially on CIFAR-100. This gap can be explained from two perspectives.

First, federated drift mainly occurs across channels and filters rather than within individual spatial kernels. The 2D FFT only analyzes isolated local  $3 \times 3$  spatial structures and therefore cannot effectively capture inter-filter divergence. In contrast, our 1D flattening strategy concatenates filters into a unified spectrum, enabling direct modeling and suppression of global cross-channel drift.

Second, the 2D FFT implementation requires executing thousands of independent small FFT operations, introducing significant memory-access and looping overhead. Our 1D FFT instead operates on contiguous flattened arrays, resulting in substantially higher computational efficiency and simpler implementation.

Overall, these results demonstrate that the success of SpecGradFilter is tightly connected to the structural organization of neural parameters. Appropriate flattening orders preserve the semantic geometry of cross-channel optimization drift, enabling frequency-domain filtering to effectively separate transferable information from client-specific bias.

**When Does Low-Frequency Filtering Help or Hurt** A natural question is whether suppressing low-frequency gradient components is always beneficial. To answer this, we investigate SpecGradFilter under different levels of decentralization and statistical heterogeneity, ranging from standard centralized training to highly heterogeneous federated learning. Our core hypothesis is that the role of low-frequency gradients fundamentally changes once optimization becomes decentralized.

*d) Centralized Learning:* In standard centralized SGD, each mini-batch is sampled from the global data distribution,

making the stochastic gradient an approximately unbiased estimator of the true optimization direction. Under this setting, low-frequency components largely encode globally consistent semantic structures and long-range optimization trends. Aggressively filtering these components therefore removes useful optimization signals and slows the learning of macro-level representations.

To verify this, we directly apply SpecGradFilter to centralized training. As shown in Table V, low-frequency suppression slightly degrades performance compared with standard SGD (e.g.,  $-0.65\%$  on CIFAR-10 and  $-1.57\%$  on CIFAR-100). This result confirms that when gradients are already globally consistent and unbiased, low-frequency filtering becomes unnecessary and may even be harmful.

*e) Federated Learning:* The optimization dynamics fundamentally change in federated learning due to decentralized local updates. Under Non-IID data distributions, local gradients become heavily biased toward client-specific objectives. As a result, the low-frequency spectrum is no longer dominated by universal semantic information, but instead becomes contaminated by client-dependent drift and accumulated optimization bias.

In this regime, suppressing low-frequency components acts as a form of spectral drift correction, removing destructive global deviations while preserving transferable high-frequency micro-structures shared across clients. Consequently, the benefit of SpecGradFilter increases as heterogeneity becomes stronger. Table V shows that the improvement consistently grows as the Dirichlet concentration parameter  $\alpha$  decreases. For example, under severe heterogeneity ( $\alpha = 0.1$ ), our method improves

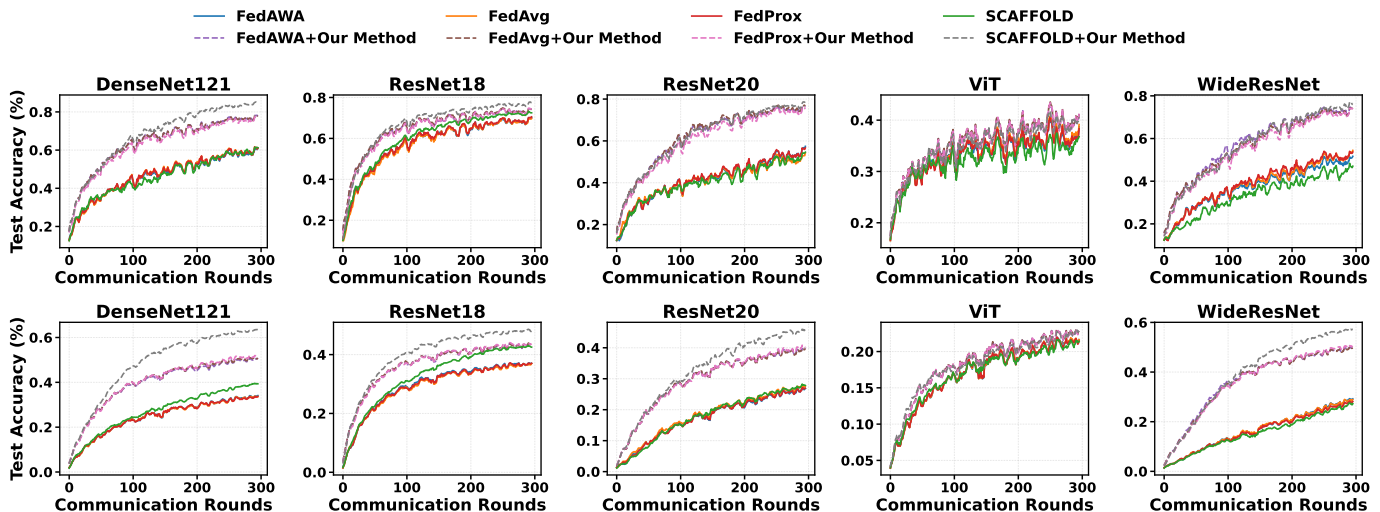


Fig. 6. Test accuracy over communication rounds under Dirichlet ( $\alpha = 0.1$ ). Solid lines denote the original federated learning methods, while dashed lines indicate the corresponding methods combined with our approach. The top row reports results on CIFAR-10, and the bottom row reports results on CIFAR-100. Each column corresponds to a different model architecture.

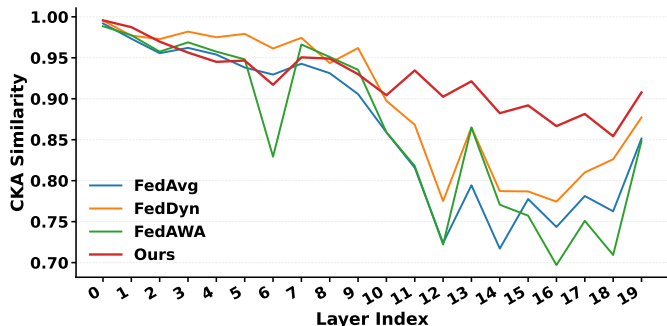


Fig. 7. Layer-wise CKA similarity among different methods on CIFAR-10 with  $\alpha = 0.1$  using ResNet-20, showing improved representation alignment.

FedAvg by +21.58% on CIFAR-10.

*f) Why Does It Still Help Under Near-IID FL:* Interestingly, SpecGradFilter remains highly effective even under near-IID federated settings ( $\alpha = 100$ ), where global label distributions are nearly identical across clients. This phenomenon suggests that the effectiveness of spectral filtering is not solely caused by statistical heterogeneity. Even in near-IID FL, each client still performs multiple local SGD updates on different mini-batch sequences before synchronization. These local optimization trajectories accumulate stochastic variance and local overfitting tendencies, producing implicit low-frequency drift across clients.

Under this perspective, low-frequency filtering also behaves as a trajectory-level regularizer, suppressing unstable large-scale optimization directions and enforcing smoother inter-client consensus dynamics. As shown in Table VI, our method still substantially outperforms strong baselines such as FedDyn and SCAFFOLD under near-IID settings. Overall, these results reveal an important property of SpecGradFilter: its effectiveness is tightly coupled with decentralized optimization dynamics rather than merely data heterogeneity itself. When gradients are globally unbiased (centralized SGD), low-frequency suppress-

ion can remove useful semantic information. However, once optimization becomes decentralized, low-frequency components increasingly encode optimization drift and client-specific bias, making spectral filtering highly beneficial.

TABLE V

PERFORMANCE COMPARISON ACROSS THE SPECTRUM OF DATA DECENTRALIZATION AND HETEROGENEITY. IN CENTRALIZED LEARNING, THE BASELINE IS STANDARD SGD; IN FEDERATED LEARNING, THE BASELINE IS FEDAVG. WHILE OUR SPECTRAL FILTERING SLIGHTLY DEGRADES PERFORMANCE IN STANDARD CENTRALIZED TRAINING (WHERE GRADIENTS ARE UNBIASED), IT PROVIDES INCREASINGLY MASSIVE GAINS AS DATA BECOMES MORE DECENTRALIZED AND HETEROGENEOUS.

Training Setting	CIFAR-10 (%)			CIFAR-100 (%)		
	Baseline	Ours	$\Delta$	Baseline	Ours	$\Delta$
Centralized Learning (Baseline: Standard SGD)						
Centralized (IID)	<b>92.87</b>	92.22	-0.65	<b>68.66</b>	67.09	-1.57
Federated Learning (Baseline: FedAvg)						
FL Near-IID ( $\alpha = 100$ )	81.28	<b>86.74</b>	+5.46	40.90	<b>49.36</b>	+8.46
FL Non-IID ( $\alpha = 5$ )	79.58	<b>86.77</b>	+7.19	38.81	<b>48.60</b>	+9.79
FL Non-IID ( $\alpha = 0.6$ )	76.72	<b>85.26</b>	+8.54	36.09	<b>46.66</b>	+10.57
FL Non-IID ( $\alpha = 0.1$ )	57.09	<b>78.67</b>	+21.58	29.15	<b>40.87</b>	+11.72

TABLE VI

TEST ACCURACY (%) ON CIFAR-10, CIFAR-100, AND TINY-IMAGENET UNDER NEAR-IID ( $\alpha = 100$ ) SETTING USING RESNET-20 WITH 100 CLIENTS, A CLIENT PARTICIPATION RATE OF 0.1, AND A FIXED COMMUNICATION BUDGET OF 300 ROUNDS.

Method	CIFAR-10	CIFAR-100	Tiny-ImageNet
FedAvg	81.28	40.90	34.00
FedProx	81.62	40.56	33.73
FedDyn	85.42	46.45	37.69
SCAFFOLD	83.22	43.31	37.18
FedCM	86.36	43.86	23.56
FedSAM	81.42	39.50	34.23
FedDisco	81.30	40.00	33.25
FedAWA	81.51	40.32	33.93
FedLWS	81.52	39.73	34.75
Our Method	86.74	49.36	38.29

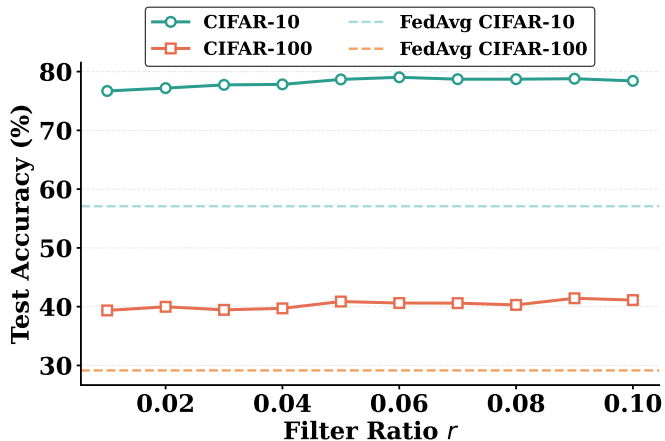


Fig. 8. Accuracy improvement of our method over FedAvg across different filter ratios.

#### D. Robustness and Generalization

**Robustness to FL Settings.** We evaluate the robustness of our method under different federated learning hyperparameters, including the number of clients, local epochs, and client participation ratio, with FedAvg, SCAFFOLD, and FedDyn as baselines (Figure 4). As the number of clients increases from 20 to 100, FedAvg and SCAFFOLD exhibit noticeable performance degradation, with FedAvg dropping from 69.4% to 57.1%, indicating aggravated client drift under larger-scale heterogeneity. In contrast, incorporating our method consistently maintains high accuracy across all client settings for all three baselines. A similar trend is observed when varying the number of local epochs or the client participation ratio: while all baselines benefit from increased local computation and participation, our method achieves substantially higher accuracy, particularly under fewer local epochs and limited client participation. Overall, these results demonstrate that frequency-based gradient filtering effectively stabilizes local optimization and improves robustness across different system configurations.

**Impact of Filtering Ratio.** We study the impact of the filter ratio on CIFAR-10 and CIFAR-100 under  $\alpha = 0.1$ , varying it from 0.01 to 0.1. As shown in Figure 8, the improvement over FedAvg remains largely stable across all values, with only minor fluctuations. This indicates that our method is robust to the choice of filter ratio, and does not require fine-tuning to achieve significant gains. CIFAR-10 exhibits slightly higher absolute improvements than CIFAR-100, but the overall trend confirms that moderate variations in the filtering strength have minimal effect on performance.

**Time Efficiency.** Although gradient filtering introduces a marginal per-round computational overhead, it is overshadowed by the substantial reduction in communication rounds required for convergence. We evaluate the practical efficiency by measuring the wall-clock time required to reach the target accuracy. As listed in Table VII, despite the slight increase in local computation, SpecGradFilter significantly accelerates the global convergence rate. In particular, both the FFT-based realization and spatial variants (LAP-D, GD) reach the target

accuracy within fewer than 80 rounds, achieving over a  $3\times$  speedup in total training time compared to FedAvg. This result highlights a critical trade-off: the minor cost of spectral filtering is a worthwhile investment for effectively slashing the communication bottleneck in heterogeneous FL environments. In addition to the measured wall-clock times, we provide a theoretical perspective on the computational cost of our method. For each layer, flattening the gradient and performing FFT followed by low-frequency suppression and inverse FFT requires  $\mathcal{O}(d \log d)$  operations, where  $d$  is the number of parameters in the layer. This overhead is much smaller than the standard backpropagation, which dominates the computational cost. We further propose two lightweight alternatives: Local Average Pooling Detrend (LAP-D) and Gaussian Detrend (GD), both of which operate in  $\mathcal{O}(d)$  time while approximating the effect of FFT-based high-pass filtering, making them highly efficient for large models or resource-constrained clients.

**Robustness Under Feature Shift.** Previous experiments mainly focused on label-distribution heterogeneity induced by Non-IID partitioning. To further evaluate the generalization ability of SpecGradFilter, we investigate a more challenging feature-shift federated setting using CIFAR-10-C and CIFAR-100-C. Unlike standard label skew, feature shift introduces systematic corruption patterns into the input space, such as blur, noise, weather effects, and contrast variations. These corruptions create strong client-specific domain styles, substantially altering the global feature statistics observed by local models.

We conduct experiments on CIFAR-10-C and CIFAR-100-C with corruption severity level 3 using a ResNet-20 backbone. To simulate a highly heterogeneous feature-shift environment, we construct a federated system with 100 clients and a low client participation ratio of 0.1. Each client is assigned only 2–3 corruption types, resulting in severe domain inconsistency across local training distributions. All methods are trained for 300 communication rounds, and results are averaged over three random seeds. The results are summarized in Table VIII.

Feature-shift federated learning introduces a fundamentally different form of heterogeneity compared with label skew. Instead of altering label distributions, corrupted domains mainly modify global appearance statistics and low-level feature distributions. These systematic domain-specific perturbations generate strong low-frequency biases in local optimization trajectories, causing severe inconsistency across clients.

Under this perspective, the low-frequency spectrum increasingly captures corruption-dependent domain styles rather than universally shared semantic information. SpecGradFilter effectively acts as a spectral domain-detrending operator that suppresses these client-specific low-frequency biases while preserving consensus semantic structures contained in higher-frequency components.

As shown in Table VIII, our method consistently achieves the best performance under severe feature shift. The improvement becomes particularly significant on CIFAR-100-C, where our method outperforms FedAvg by more than 10%. Notably, the gain further enlarges under the challenging regime of low client participation and highly fragmented corruption distributions, demonstrating that SpecGradFilter remains effective even when

TABLE VII

TRAINING EFFICIENCY COMPARISON (SECONDS) ON NVIDIA TESLA A40 WITH RESNET-20. COMPARISON OF COMMUNICATION ROUNDS ( $R$ ), AVERAGE TIME PER ROUND ( $T_{rnd}$ ), AND TOTAL TRAINING TIME ( $T_{total}$ ) TO REACH THE TARGET ACCURACY ACHIEVED BY FEDAVG (57% ON CIFAR-10, 27% ON CIFAR-100, AND 25% ON TINY-IMAGENET). “†” INDICATES FAILURE TO CONVERGE TO THE TARGET.

Method	Dataset								
	CIFAR-10			CIFAR-100			Tiny-ImageNet		
	$T_{rnd}$	$R$	$T_{total}$	$T_{rnd}$	$R$	$T_{total}$	$T_{rnd}$	$R$	$T_{total}$
FedAvg	<b>5.51</b>	300	1653.00	<b>5.30</b>	255	1351.50	<b>24.89</b>	270	6720.30
FedProx	5.86	255	1494.00	5.83	262	1527.46	26.46	255	6747.30
FedDyn	6.10	167	1018.70	5.80	180	1044.00	26.05	194	5053.70
SCAFFOLD	5.76	299	1722.20	5.75	262	1506.50	26.73	251	6709.23
FedSAM	8.09	271	2192.40	8.56	284	2431.04	36.02	293	10553.86
FedCM	6.04	128	773.10	5.73	284	1627.32	†	†	†
FedDisco	5.54	254	1407.20	5.79	270	1563.30	25.98	299	7768.02
FedAWA	5.52	255	1407.60	5.48	262	1435.76	25.34	270	6841.80
FedLWS	5.62	255	1433.10	5.33	270	1439.10	24.86	270	6712.20
FedAvg + LAP-D	5.97	97	579.10	5.86	128	750.08	25.34	108	2736.72
FedAvg + GD	6.66	79	526.10	6.42	93	597.06	25.98	98	2546.04
FedAvg + FFT	6.38	<b>75</b>	<b>478.50</b>	6.25	<b>86</b>	<b>537.50</b>	25.52	<b>93</b>	<b>2373.36</b>

TABLE VIII

PERFORMANCE UNDER FEATURE-SHIFT FEDERATED LEARNING ON CIFAR-10-C AND CIFAR-100-C (SEVERITY LEVEL 3) USING RESNET-20. WE REPORT MEAN TEST ACCURACY (%) OVER THREE RANDOM SEEDS UNDER A CHALLENGING SETTING WITH 100 CLIENTS AND CLIENT PARTICIPATION RATIO  $R = 0.1$ .

Method	CIFAR-10-C	CIFAR-100-C
FedAvg	62.11 $\pm$ 0.78	26.18 $\pm$ 0.53
FedDyn	68.74 $\pm$ 1.13	31.83 $\pm$ 0.41
FedCM	76.86 $\pm$ 0.34	23.45 $\pm$ 1.18
SCAFFOLD	61.25 $\pm$ 1.01	25.95 $\pm$ 0.63
FedAvg + Our Method	<b>77.68 <math>\pm</math> 0.42</b>	<b>37.04 <math>\pm</math> 0.28</b>

heterogeneity originates from feature-level domain shifts rather than label imbalance.

These results suggest that the benefit of spectral filtering is not limited to conventional Non-IID label skew, but extends more broadly to decentralized optimization scenarios where client-specific low-frequency biases dominate local updates.

**NLP and Medical Imaging Task.** Table IX shows the test accuracy across various federated learning algorithms on both NLP and medical imaging tasks [31] under different Dirichlet heterogeneity levels. For the Yahoo! Answers dataset, we observe that applying our method on top of FedAvg, SCAFFOLD, or FedAWA consistently improves performance under both  $\alpha = 0.6$  and  $\alpha = 0.1$ , indicating that low-frequency gradient suppression effectively improves client alignment and enhances accuracy even in NLP tasks. Similarly, on the BloodMNIST dataset, our method also leads to significant performance gains across all federated algorithms, particularly under more challenging heterogeneity settings. These results further highlight the robustness of our approach, demonstrating its effectiveness not only in NLP tasks but also in medical image classification.

**Realistic Federated Setting.** This section evaluates the proposed method under a realistic federated learning setting, where only a fraction of clients participate in each communication round. Table X reports the test accuracy on FEMNIST

TABLE IX

TEST ACCURACY (%) UNDER DIFFERENT DIRICHLET HETEROGENEITY LEVELS.

Method	Yahoo Answer		BloodMNIST	
	$\alpha = 0.6$	$\alpha = 0.1$	$\alpha = 0.6$	$\alpha = 0.1$
FedAvg	47.90	22.00	91.05	84.18
<b>+ Our Method</b>	<b>50.90</b>	<b>25.61</b>	<b>94.12</b>	<b>90.38</b>
SCAFFOLD	54.13	19.13	90.91	81.99
<b>+ Our Method</b>	<b>55.73</b>	<b>21.03</b>	<b>93.48</b>	<b>88.25</b>
FedAWA	47.84	22.56	91.49	83.83
<b>+ Our Method</b>	<b>51.08</b>	<b>25.83</b>	<b>94.15</b>	<b>91.02</b>

TABLE X

TEST ACCURACY (%) ON FEMNIST UNDER DIFFERENT CLIENT ACTIVE RATIOS.

Method	Active Ratio = 0.05	Active Ratio = 0.1
FedAvg	78.95	78.02
<b>+ Our Method</b>	<b>81.58</b>	<b>82.56</b>
SCAFFOLD	75.16	77.48
<b>+ Our Method</b>	<b>77.57</b>	<b>82.34</b>
FedAWA	79.00	78.46
<b>+ Our Method</b>	<b>81.54</b>	<b>82.03</b>

under different client active ratios. The results show that our method consistently improves performance over all baselines across different participation rates. Notably, even under low client participation, the proposed approach maintains stable and reliable performance gains, demonstrating its robustness in realistic federated scenarios with partial and dynamic client availability.

## VI. CONCLUSION

We present SpecGradFilter, a communication-efficient method to mitigate client drift in federated learning via spectral analysis of model gradients. By treating gradients as structured signals, we identify the Spectral Bias of Drift, showing that

inter-client divergence concentrates in low-frequency components, especially under severe heterogeneity. SpecGradFilter suppresses these components during local updates, improving inter-client alignment while preserving task-relevant high-frequency information. Experiments on diverse datasets and models show consistent gains over drift-mitigation baselines, with faster convergence and higher accuracy. Future work includes adaptive spectral filtering and extending this framework to large-scale models such as LLMs, where heterogeneity and optimization instability are more pronounced.

## VII. ACKNOWLEDGMENT

This work of Liyang Yuan and Dandan Guo was supported in part by the National Natural Science Foundation of China (NSFC) under Grant 62306125.

Generative AI tools (e.g., ChatGPT) were used to assist with language refinement. All scientific content, methodology, experimental results, and conclusions were developed and verified by the authors.

## REFERENCES

- [1] B. McMahan, E. Moore, D. Ramage, S. Hampson, and B. A. y Arcas, "Communication-efficient learning of deep networks from decentralized data," in *Proceedings of the 20th International Conference on Artificial Intelligence and Statistics (AISTATS)*, 2017.
- [2] S. Wang, F. Roosta, P. Xu, and M. W. Mahoney, "Giant: Globally improved approximate newton method for distributed optimization," *Advances in neural information processing systems*, vol. 31, 2018.
- [3] M. Li, D. G. Andersen, A. Smola, and K. Yu, "Communication efficient distributed machine learning with the parameter server," *Advances in neural information processing systems*, vol. 27, 2014.
- [4] F. N. Iandola, M. W. Moskewicz, K. Ashraf, and K. Keutzer, "Firecaffe: Near-linear acceleration of deep neural network training on compute clusters," *2016 IEEE Conference on Computer Vision and Pattern Recognition (CVPR)*, pp. 2592–2600, 2015. [Online]. Available: <https://api.semanticscholar.org/CorpusID:8480861>
- [5] X. Yang, R. Dai, Y. Zhang, A. Li, T. Liu, and B. Han, "Co-boosting++: Coupled optimization of data and ensemble for one-shot federated learning," *IEEE Transactions on Pattern Analysis and Machine Intelligence*, 2026.
- [6] A. Khaled, K. Mishchenko, and P. Richtárik, "Tighter theory for local sgd on identical and heterogeneous data," in *International Conference on Artificial Intelligence and Statistics*, 2019. [Online]. Available: <https://api.semanticscholar.org/CorpusID:210839089>
- [7] B. Woodworth, K. K. Patel, S. U. Stich, Z. Dai, B. Bullins, H. B. McMahan, O. Shamir, and N. Srebro, "Is local sgd better than minibatch sgd?" in *Proceedings of the 37th International Conference on Machine Learning*, ser. ICML'20. JMLR.org, 2020.
- [8] T. Li, A. K. Sahu, A. Talwalkar, and V. Smith, "Federated learning: Challenges, methods, and future directions," *IEEE Signal Processing Magazine*, vol. 37, no. 3, pp. 50–60, 2020.
- [9] Z. Fan, Y. Wang, J. Yao, L. Lyu, Y. Zhang, and Q. Tian, "Fedskip: Combatting statistical heterogeneity with federated skip aggregation," in *2022 IEEE International Conference on Data Mining (ICDM)*, 2022, pp. 131–140.
- [10] D. A. E. Acar, Y. Zhao, R. Matas, M. Mattina, P. Whatmough, and V. Saligrama, "Federated learning based on dynamic regularization," in *International Conference on Learning Representations*, 2021. [Online]. Available: <https://openreview.net/forum?id=B7v4QMR6Z9w>
- [11] Q. Li, B. He, and D. Song, "Model-contrastive federated learning," in *2021 IEEE/CVF Conference on Computer Vision and Pattern Recognition (CVPR)*, 2021, pp. 10 708–10 717.
- [12] Y. Shi, K. Wei, L. Shen, Y. Liu, X. Wang, B. Yuan, and D. Tao, "Towards the flatter landscape and better generalization in federated learning under client-level differential privacy," *IEEE Transactions on Pattern Analysis and Machine Intelligence*, 2025.
- [13] T. Li, A. K. Sahu, M. Zaheer, M. Sanjabi, A. Talwalkar, and V. Smith, "Federated optimization in heterogeneous networks," *Proceedings of Machine learning and systems*, vol. 2, pp. 429–450, 2020.
- [14] S. P. Karimireddy, S. Kale, M. Mohri, S. Reddi, S. Stich, and A. T. Suresh, "Scaffold: Stochastic controlled averaging for federated learning," in *International conference on machine learning*. PMLR, 2020, pp. 5132–5143.
- [15] R. Ye, M. Xu, J. Wang, C. Xu, S. Chen, and Y. Wang, "Feddisco: federated learning with discrepancy-aware collaboration," in *Proceedings of the 40th International Conference on Machine Learning*, ser. ICML'23. JMLR.org, 2023.
- [16] C. Shi, H. Zhao, B. Zhang, M. Zhou, D. Guo, and Y. Chang, "Fedawa: Adaptive optimization of aggregation weights in federated learning using client vectors," in *Proceedings of the IEEE/CVF Conference on Computer Vision and Pattern Recognition (CVPR)*, 2025.
- [17] N. Rahaman, A. Baratin, D. Arpit, F. Dräxler, M. Lin, F. A. Hamprecht, Y. Bengio, and A. C. Courville, "On the spectral bias of neural networks," in *International Conference on Machine Learning*, 2018. [Online]. Available: <https://api.semanticscholar.org/CorpusID:53012119>
- [18] Z.-Q. J. Xu, Y. Zhang, T. Luo, Y. Xiao, and Z. Ma, "Frequency principle: Fourier analysis sheds light on deep neural networks," *ArXiv*, vol. abs/1901.06523, 2019. [Online]. Available: <https://api.semanticscholar.org/CorpusID:58981616>
- [19] L. Yi, X. Shi, N. Wang, J. Zhang, G. Wang, and X. Liu, "Fedpe: Adaptive model pruning-expanding for federated learning on mobile devices," *IEEE Transactions on Mobile Computing*, vol. 23, no. 11, pp. 10 475–10 493, 2024.
- [20] Q. Yang, L. Chen, M. Xue, and S. Li, "Tackling resource-constrained and data-heterogeneity in federated learning with double-weight sparse pack," in *Proceedings of the AAAI Conference on Artificial Intelligence*, vol. 40, no. 32, 2026, pp. 27 592–27 600.

- [21] L. Gao, H. Fu, L. Li, Y. Chen, M. Xu, and C.-Z. Xu, “Feddc: Federated learning with non-iid data via local drift decoupling and correction,” in *Proceedings of the IEEE/CVF Conference on Computer Vision and Pattern Recognition (CVPR)*. IEEE Computer Society, June 2022, pp. 10 112–10 121.
- [22] J. Zhang, Z. Li, B. Li, J. Xu, S. Wu, S. Ding, and C. Wu, “Certified robustness of joint embedding,” in *Proceedings of the 39th International Conference on Machine Learning*, ser. Proceedings of Machine Learning Research, K. Chaudhuri, S. Jegelka, L. Song, C. Szepesvári, G. Niu, and S. Sabato, Eds., vol. 162. PMLR, 2022, pp. 26 311–26 329.
- [23] Z. Li, T. Lin, X. Shang, and C. Wu, “Revisiting weighted aggregation in federated learning with neural networks,” in *Proceedings of the 40th International Conference on Machine Learning*, ser. ICML’23. JMLR.org, 2023.
- [24] Y.-H. Chan, R. Zhou, R. Zhao, Z. Jiang, and E. Ngai, “Internal cross-layer gradients for extending homogeneity to heterogeneity in federated learning,” in *International Conference on Learning Representations*, vol. 2024, 2024, pp. 1983–2011.
- [25] L. Wang, W. Wu, J. Zhang, H. Liu, G. Bosilca, M. Herlihy, and R. Fonseca, “Fft-based gradient sparsification for the distributed training of deep neural networks,” in *Proceedings of the 29th International Symposium on High-Performance Parallel and Distributed Computing*, 2020, pp. 113–124.
- [26] H. Shi, W. Xie, H. Ye, D. Li, J. Ma, Y. Li, and L. Fang, “High-energy concentration for federated learning in frequency domain,” 2025. [Online]. Available: <https://arxiv.org/abs/2509.12630>
- [27] C. Palihawadana, N. Wiratunga, A. Wijekoon, and H. Kalutarage, “Fedft: Improving communication performance for federated learning with frequency space transformation,” 2024. [Online]. Available: <https://arxiv.org/abs/2409.05242>
- [28] A. Krizhevsky and G. Hinton, “Learning multiple layers of features from tiny images,” University of Toronto, Toronto, Ontario, Tech. Rep. 0, 2009. [Online]. Available: <https://www.cs.toronto.edu/~kriz/learning-features-2009-TR.pdf>
- [29] S. U. CS231N, “Tiny imagenet visual recognition challenge,” <http://cs231n.stanford.edu/>, 2015.
- [30] S. Caldas, S. M. K. Duddu, P. Wu, T. Li, J. Konečný, H. B. McMahan, V. Smith, and A. Talwalkar, “Leaf: A benchmark for federated settings,” 2019. [Online]. Available: <https://arxiv.org/abs/1812.01097>
- [31] J. Yang, R. Shi, D. Wei, Z. Liu, L. Zhao, B. Ke, H. Pfister, and B. Ni, “Medmnist v2-a large-scale lightweight benchmark for 2d and 3d biomedical image classification,” *Scientific data*, vol. 10, no. 1, p. 41, 2023.
- [32] J. Xu, S. Wang, L. Wang, and A. C.-C. Yao, “Fedcm: Federated learning with client-level momentum,” *ArXiv*, vol. abs/2106.10874, 2021. [Online]. Available: <https://api.semanticscholar.org/CorpusID:235490679>
- [33] D. Caldarola, B. Caputo, and M. Ciccone, “Improving generalization in federated learning by seeking flat minima,” in *European Conference on Computer Vision*. Springer, 2022, pp. 654–672.
- [34] Z. Qu, X. Li, R. Duan, Y. Liu, B. Tang, and Z. Lu, “Generalized federated learning via sharpness aware minimization,” in *International conference on machine learning*. PMLR, 2022, pp. 18 250–18 280.
- [35] C. Shi, J. Li, H. Zhao, D. Guo, and Y. Chang, “Fedlws: Federated learning with adaptive layer-wise weight shrinking,” in *International Conference on Learning Representations (ICLR)*, 2025.
- [36] K. He, X. Zhang, S. Ren, and J. Sun, “Deep residual learning for image recognition,” in *2016 IEEE Conference on Computer Vision and Pattern Recognition (CVPR)*, 2016, pp. 770–778.
- [37] Y. Sun, L. Shen, S. Chen, L. Ding, and D. Tao, “Dynamic regularized sharpness aware minimization in federated learning: Approaching global consistency and smooth landscape,” in *International Conference on Machine Learning*. PMLR, 2023, pp. 32 991–33 013.
- [38] Z. Fan, S. Hu, J. Yao, G. Niu, Y. Zhang, M. Sugiyama, and Y. Wang, “Locally estimated global perturbations are better than local perturbations for federated sharpness-aware minimization,” in *International Conference on Machine Learning*, 2024.
- [39] Y. Wu and K. He, “Group normalization,” in *Computer Vision – ECCV 2018: 15th European Conference, Munich, Germany, September 8-14, 2018, Proceedings, Part XIII*. Berlin, Heidelberg: Springer-Verlag, 2018, p. 3–19. [Online]. Available: [https://doi.org/10.1007/978-3-030-01261-8\\_1](https://doi.org/10.1007/978-3-030-01261-8_1)

**Liyang Yuan** is currently working toward the M.S. degree with the School of Artificial Intelligence, Jilin University, Changchun, China. He received the B.S. degree in artificial intelligence from Ludong University, Yantai, China, in 2024. His current research interests include federated learning and client data heterogeneity.



**Yibo Yang** is a research scientist at KAUST. He obtained his Ph.D. degree from Peking University in 2021. He conducted research at JD Explore Academy and the University of Oxford. His research interests lie in machine learning and computer vision. He has published more than 40 publications in top-tier journals and conferences with more than 4000 citations. He was awarded the CAAI Wuwenjun AI Science and Technology Award, First Prize of Natural Science (5-th contributor) and the CAAI Wuwenjun Outstanding Ph.D. Dissertation Award. He was also



awarded the first prize in BMTT challenge 2021, the Innovative Award in MS COCO challenge 2019, and the Runner-up Award in MS COCO challenge 2018. He has served as Area Chair for NeurIPS, ICML, and ICLR.



**Dandan Guo** is currently a Professor with the School of Artificial Intelligence, Jilin University, Changchun, China. Since 2025, she has also been a Visiting Faculty at King Abdullah University of Science and Technology (KAUST), Saudi Arabia. She received the Ph.D. degree in electronic engineering from Xidian University, Xi'an, China, in 2020. From 2020 to 2022, she was a Postdoctoral Researcher with The Chinese University of Hong Kong, Shenzhen, China. Her current research interests include advanced machine learning, federated learning, large language models (LLMs), and self-improving AI agents.



**Peter Richtárik** is a professor of Computer Science at KAUST, Saudi Arabia, where he leads the Optimization and Machine Learning Lab. Through his work on randomized and distributed optimization algorithms, he has contributed to the foundations of machine learning and optimization. He is one of the original developers of Federated Learning. Prof Richtárik's works attracted international awards, including the Charles Broyden Prize, SIAM SIGEST Best Paper Award, and a Distinguished Speaker Award at the 2019 International Conference on Continuous Optimization. He serves as an Area Chair for leading machine learning conferences, including NeurIPS, ICML and ICLR, and is an Action Editor of JMLR, and Associate Editor of Numerische Mathematik, and Optimization Methods and Software.



**Zhouchen Lin** (M'00–SM'08–F'18) is currently a Boya Special Professor with the State Key Laboratory of General Artificial Intelligence, School of Intelligence Science and Technology, Peking University. He received the Ph.D. degree in applied mathematics from Peking University in 2000. His research interests include machine learning and numerical optimization. He has published over 310 papers, collecting more than 45000 Google Scholar citations. He is a Fellow of the IAPR, the IEEE, the AAIA and the CSIG.